12th International Symposium on Turbulence and Shear Flow Phenomena (TSFP12)
Osaka, Japan (Online), July 19-22, 2022

LOW-ORDER MODELLING OF TURBULENT QUASI-CYCLIC BEHAVIOUR AND SUDDEN RELAMINARISATION

Ryo Araki
LMFA
École Centrale de Lyon
69134 Écully cedex, France
Graduate School of Engineering Science
Osaka University
1-3 Machikaneyama, Toyonaka, Osaka 560-8531, Japan
araki.ryo@ec-lyon.fr

Wouter J. T. Bos
LMFA
École Centrale de Lyon, CNRS, Univ Lyon
69134 Écully cedex, France
wouter.bos@ec-lyon.fr

Susumu Goto
Graduate School of Engineering Science
Osaka University
1-3 Machikaneyama, Toyonaka, Osaka 560-8531, Japan
s.goto.es@osaka-u.ac.jp

ABSTRACT

We propose a three-equation model which reproduces the quasi-cyclic behaviour of turbulent flow [Araki *et al.* (2022)]. We examine a 3D flow driven by steady forcing at various Reynolds numbers (Re) to find a perfectly time-periodic flow at a specific low Re and quasi-cyclic flow at higher Re. The two states are continuously connected when changing Re. A mode-by-mode analysis of the periodic flow allows us to formulate the minimal model, which describes the evolution of three families of scales with their nonlinear interactions, dissipation, and driving terms. By calibrating the model parameters to the DNS results, when possible, we find a qualitatively similar periodic solution to the DNS. By increasing the "Reynolds number" of the model, we find permanent chaos, which we compare to turbulence. The same model also reproduces probabilistic transitions between chaotic and steady states for the different parameter sets. The scaling of this sudden relaminarisation agrees with the ones observed in turbulence to some extent. We consider that our minimal model reproduces several key properties of turbulence.

BACKGROUND

Quasi-Cyclic Behaviour (QCB) is observed in many turbulent flows and is sometimes related to the energy cascade mechanism. For example, QCB is observed in periodic box turbulence driven by a steady forcing and found to be associated with vortex stretching of hierarchical coherent vortical structures responsible for the energy cascade from large to small scales (Goto *et al.*, 2017). Furthermore, QCB is associated with the concept of unstable periodic orbits and has been extensively studied (Lucas & Kerswell, 2017; van Veen *et al.*, 2019). Another important example is the self-sustaining process in near-wall turbulence (Waleffe, 1997).

This study finds a non-trivial periodic flow in Direct Numerical Simulation (DNS), using a time-independent Taylor–Green forcing. The features of the periodic flow are similar to developed turbulence at higher Reynolds numbers. Our goal is to illustrate the similarity between the temporal dynamics of the periodic and turbulent flow and model them with a minimal degree of freedom to understand the origin of the QCB.

Thereto, we conduct DNS of the Navier-Stokes equations,

$$\begin{cases} \partial_t \mathbf{u} + (\mathbf{u}\cdot\nabla)\mathbf{u} = -\nabla p + \nu\nabla^2\mathbf{u} + \mathbf{f}, & (1) \\ \mathbf{f} = (-f_0 \sin x \cos y, f_0 \cos x \sin y, 0), & (2) \end{cases}$$

along with the incompressibility condition $\nabla\cdot\mathbf{u} = 0$. Here, $\mathbf{u}$, p, and $\mathbf{f}$ denote velocity, pressure, and steady Taylor–Green body force fields, respectively. The kinematic viscosity ν is the control parameter of the flow and we define the Reynolds number $\mathrm{Re} \equiv \sqrt{f_0}/|\mathbf{k}_f|^{3/2}\nu$ with the forced wavenumber $\mathbf{k}_f = (1,1,0)$. We set the forcing coefficient f_0 to unity.

We summarise both 3D Periodic Flow (3DPF) at $\mathrm{Re} = 5.83$ and turbulence at $\mathrm{Re} = 29.7$ in Fig. 1. Visualisations of vorticity magnitude (Fig. 1 (a,c)) depict similar spatial structures for both Re, namely, the forcing-induced large-scale columnar vortices and smaller vortices in antiparallel orientation. Here, low-pass filtered quantity is defined by $\mathbf{u}^<(\mathbf{x}) \equiv \int \mathrm{d}\mathbf{r}\, G(r/\sigma)\mathbf{u}(\mathbf{x}+\mathbf{r})$, where $G(r/\sigma)$ is Gaussian function and we set $\sigma = \sqrt{2}|\mathbf{k}_f| = 2$. Parametric time series of energy input rate $P \equiv \langle \mathbf{f}\cdot\mathbf{u}\rangle$ and energy dissipation rate $\varepsilon = \nu\langle|\omega|^2\rangle$, where $\omega = \nabla\times\mathbf{u}$ and $\langle\cdot\rangle$ is the spatial average, show counterclockwise cycle in the 3DPF (Fig. 1 (b)). Here, the time series are normalised by the characteristic time scale $T \equiv \left(|\mathbf{k}_f| f_0\right)^{-1} = 0.840$, where $|\mathbf{k}_f| = \sqrt{2}$ and $f_0 = 1$. The turbulent time series in Fig. 1 (d) also displays intrinsic QCB after a phase-averaging process. See Araki *et al.* (2022) for the detail of this procedure. We note that for intermediate $5.83 < Re < 29.7$, we observe continuously changing phase-averaged $\langle P\rangle_{\mathrm{phase}}$–$\langle\varepsilon\rangle_{\mathrm{phase}}$ plots from Fig. 1 (b) to Fig. 1 (d).

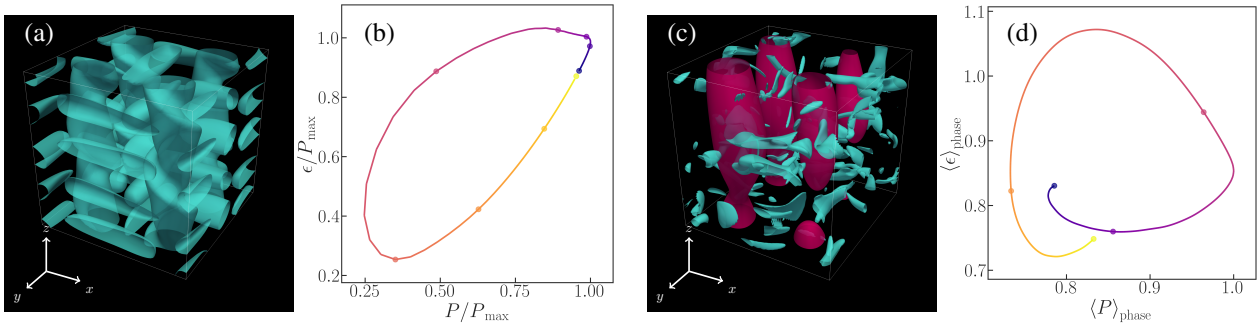

Figure 1. (a,c) Visualisations of vortical structures and (b,d) parametric time series of energy dissipation rate $\varepsilon(t)$ against energy input rate $P(t)$ in (a,b) low Reynolds number periodic flow at $\mathrm{Re} = 5.83$ and (c,d) high Reynolds number turbulent flow at $\mathrm{Re} = 29.7$. Visualisations show isosurfaces of (a) $|\omega|$ in cyan and (c) $|\omega|$ in cyan and low-pass filtered $|\omega^<|$ in red. Parametric time series show (b) original time series for $40T$ and (d) phase averaged time series for $20T$. The original time series in panel (b) are normalised by the maximum $P_{\max}$ of $P(t)$. The phase-averaged time series are also normalised during the process. Thus the maximum of $\langle P\rangle_{\text{phase}}$ is also unity. Dark to light colours represent the time evolution, and the gap between two consecutive dots denotes $5T$.

Thus, we conclude that the current flow exhibits QCB regardless of the Reynolds number (See also Fig. 12 of Goto *et al.* (2017) for results with three different forcing schemes at higher Re).

THREE-EQUATION MODEL

We consider a minimal model to reproduce such robust QCB irrespective of Re. By investigating the Fourier mode dynamics of the 3DPF, we find a few modes energetically dominate the 3DPF. Thus, we can decompose the flow into three "families" of Fourier modes. Figure 2 shows the schematic of such a grouping. The first family corresponds to the forced mode $\mathbf{k}_f = (1,1,0)$. Next, we define the primary energetic scale with six Fourier modes. The forced plus the primary scales (seven Fourier modes in total) reproduce more than 98 % of the time average of energy $E = \langle|\mathbf{u}|^2\rangle/2$ in the 3DPF. Last, we introduce the secondary scale, which consists of the rest of the Fourier modes. Although the energy of these modes (large-scale representative) is small, their enstrophy (small-scale representative) is non-negligible.

After assessing the possible triad interactions among these three scales (triangles in Fig. 2), we propose the following three-equation model,

$$\begin{cases} \mathrm{d}_t X = -A_1 Y^2 + A_3 YZ - \nu K_X^2 X + F, \\ \mathrm{d}_t Y = +A_1 XY - A_2 Z^2 + A_4 XZ - \nu K_Y^2 Y, \\ \mathrm{d}_t Z = +A_2 YZ - (A_3 + A_4) XY - \nu K_Z^2 Z, \end{cases} \tag{3}$$

where X, Y, and Z denote the characteristic velocity amplitude of the forced, primary, and secondary scales, respectively. The right-hand side of Eq. (3) consists of nonlinear terms with coefficients A_i with $i = 1$–4, viscous damping terms multiplied by νK_α^2 where K_α is a characteristic scale factor with $\alpha = \{X, Y, Z\}$, and a forcing term F acting solely on the forced scale. We define the Reynolds number of the model by $\mathrm{Re} \equiv 1/\nu$ to analyse the model. Note that sign of A_i is set to satisfy the detailed energy conservation in the triad interactions. The coefficients A_1 and A_2 represent the scale-local forward energy transfer from X to Y and Y to Z, respectively. The remaining A_3 and A_4 terms represent non-local interactions that give the model additional freedom in the parameter space.

We fit six of nine parameters of the model by DNS of 3DPF. We investigate the energy equation of the model and compare each term with the DNS result to estimate the parameters. The scale-local nonlinear coefficients A_1 and A_2 are compared to the average energy transfer from the forced mode to the primary energetic modes while ignoring the scale non-local terms, $A_3 = A_4 = 0$. The viscous coefficients K_α^2 are evaluated by the time average of $\varepsilon_\alpha/2\nu E_\alpha$, where E_α and ε_α are energy and energy dissipation rate of scale $\alpha = \{X, Y, Z\}$ of the 3DPF. The forcing term F is defined from $P/\sqrt{2E_X}$. The obtained parameters are, $A_1 = 0.4$, $A_2 = 4$, $F = 0.7$, $K_X^2 = 2$, $K_Y^2 = 5$, and $K_Z^2 = 15$. This analysis leaves two unset parameters A_3 and A_4. The model has one control parameter $\mathrm{Re} \equiv 1/\nu$.

RESULTS

By setting $A_3 = -0.5$ and $A_4 = -0.95$, we obtain a bifurcation diagram shown in Fig. 3 (a). The first bifurcation is supercritical from steady to periodic solutions at $\mathrm{Re} \approx 12.0$, followed by a subcritical one to a more complex periodic solution at $\mathrm{Re} \approx 14.0$. Then, we identify a critical Re of the permanently chaotic solution at $14.060 < \mathrm{Re}_{\mathrm{cr}} < 14.061$. We realize that the periodic and chaotic solutions take similar orbits in the phase space as shown in Fig. 3 (b). Thus, the chaotic orbit exhibits QCB.

We compare the 3DPF and the periodic solution of the model in Fig. 4 by computing two quantities. One is the energy of the forced mode from which we subtract the laminar base flow, defined by $E_{X-X_0} \equiv |\mathbf{u}(\mathbf{k}_f) - \mathbf{f}/2\nu k_f^2|^2/2$ for the DNS and $E_{X-X_0} \equiv (X - F\,\mathrm{Re}/K_X^2)^2/2$ for the model. The other is the energy contained by the remaining modes E_{Y+Z}. In the DNS, E_{Y+Z} means the energy of the flow without the forced mode $\mathbf{k}_f$. In the model, $E_{Y+Z} \equiv Y^2/2 + Z^2/2$. Figure 4 shows the qualitatively same periodic fluctuations in terms of the relation of amplitude and phase of peaks between two quantities. Notably, both E_{X-X_0} and E_{Y+Z} show exponential growth and decay, reminiscent of the predator-prey dynamics. Although our three-equation model (3) is different from the standard two-species Lotka-Volterra equations, this similarity suggests the link between the QCB in turbulent flow and a kind of predator-prey relation between large and small scale vortex structures. We stress here that the model without the non-local triad, $A_3 = 0$, $A_4 = 0$, or $A_3 + A_4 = 0$, does not excite permanent fluctuations, indicating the necessity of the

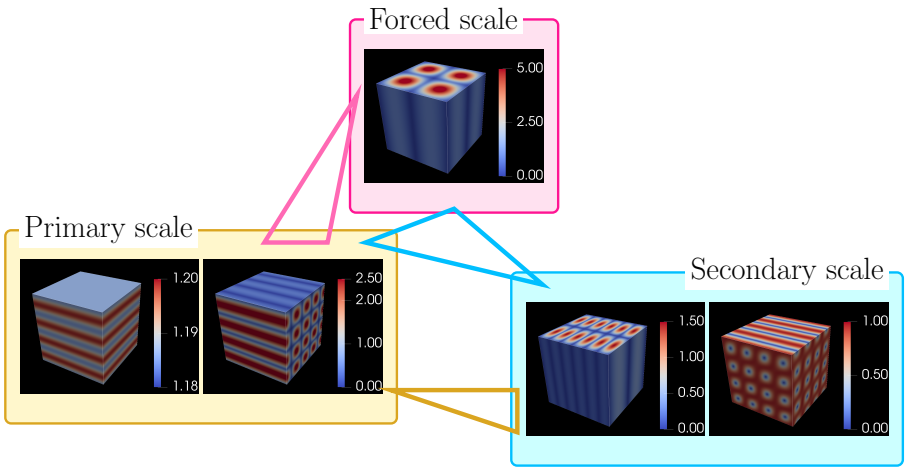

Figure 2. Schematic of three different scales. We visualize $|\omega|$ distributions of typical Fourier modes in each scale. The forced wave vector is $\mathbf{k}_f = (1,1,0)$. In the primary scale, we visualize $\mathbf{k} = (0,0,2)$ and $(0,2,2)$ modes. For the secondary scale, we visualize $\mathbf{k} = (3,1,0)$ and $(2,2,2)$ modes for example. Triangles denote triad interactions between different scales satisfying triad interaction conditions, $\mathbf{k}+\mathbf{p}+\mathbf{q} = \mathbf{0}$.

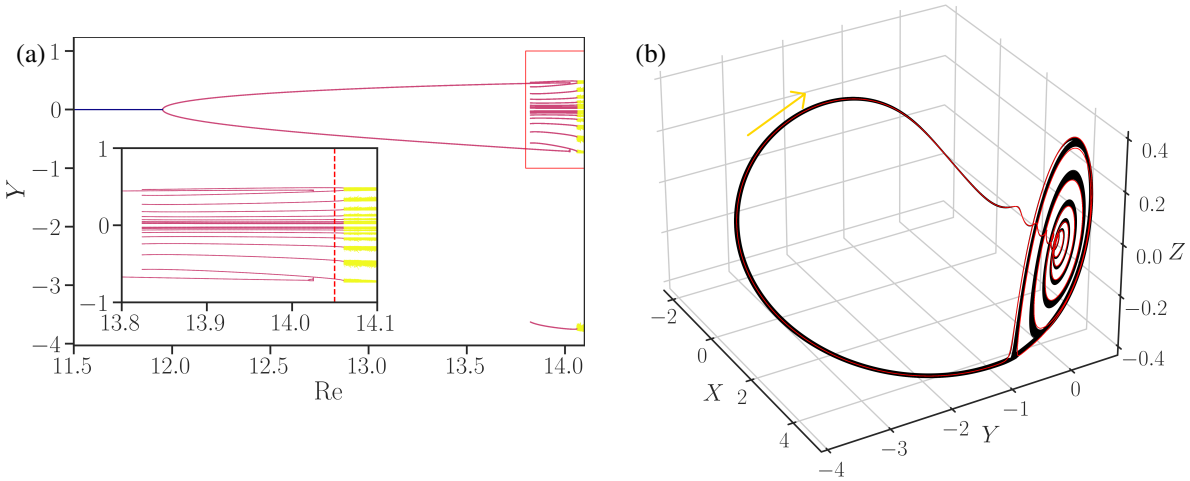

Figure 3. (a) Bifurcation diagram of the model (3) by the local extrema of Y. See main text for the parameter set-up. Blue, red, and yellow points denote steady, periodic, and chaotic solutions, respectively. Inset: close-up in the range shown by the red rectangle in the main plot. (b) Periodic (red, Re = 14.05 shown by the red vertical dashed line in panel (a)) and chaotic (black, Re = 14.1) orbits of the model (3). The chaotic orbit is tracked over 100 periods. The yellow arrow indicates the direction of the orbit.

scale non-local triad interactions to maintain the QCB. Note that we observe fast oscillations in the model (Fig. 4 (b)) and not in the DNS result (Fig. 4 (a)). By the mode-by-mode analysis, we find that there are also rapid fluctuations in specific Fourier modes of the 3DPF. However, such behaviour is compensated between the symmetric modes and does not appear in Fig. 4 (b).

Another intriguing property of the model is that it exhibits a sudden transition from a chaotic to steady states as shown in Fig. 5 (a). Here, we employ a different parameter set-up ($A_3 = 0.4$ and $A_4 = -0.5$ with other parameters being as same as in Fig. 3 and Fig. 4 (b)). This probabilistic process reminds us of the sudden relaminarisation observed in linearly forced box turbulence (Linkmann & Morozov, 2015). We compute the survival probability $P_{\mathrm{Re}}(t)$ of how likely the solution in a chaotic regime at a given time t to plot in Fig. 5 (b). We find the exponential scaling with the characteristic time scale τ,

$$P_{\mathrm{Re}}(t) = c\exp[-t/\tau(\mathrm{Re})], \tag{4}$$

in which τ also displays exponential scaling against Re,

$$\tau(\mathrm{Re}) = c'\exp[a\,\mathrm{Re}], \tag{5}$$

as shown in Fig. 5 (b) inset. Although Eq. (4) is consistent with the literature (Linkmann & Morozov (2015)), the exponential scaling of $\tau(\mathrm{Re})$ by Eq. (5) crucially differs from a super-exponential behaviour observed in Linkmann & Morozov (2015). We speculate that this reflects the minimum degree of freedom in the model.

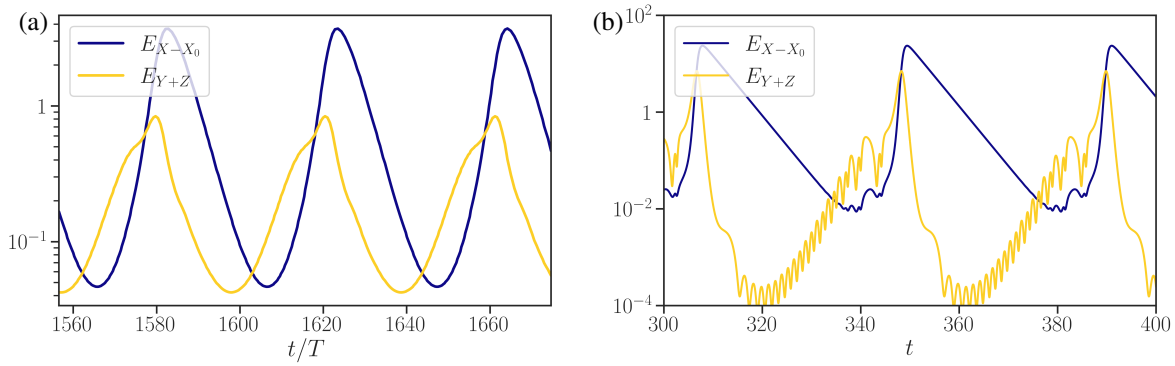

Figure 4. Time series of fluctuating energy $E_{X-X_0}(t)$ of the forced scale and residual energy $E_{Y+Z}(t)$ of (a) 3DPF of the Navier-Stokes equations (1) and (b) the model (3) at $\mathrm{Re} = 14.05$. See main text for the parameter set-up and the definition of the quantities. Note that time in panel (a) is normalised by the characteristic time scale T.

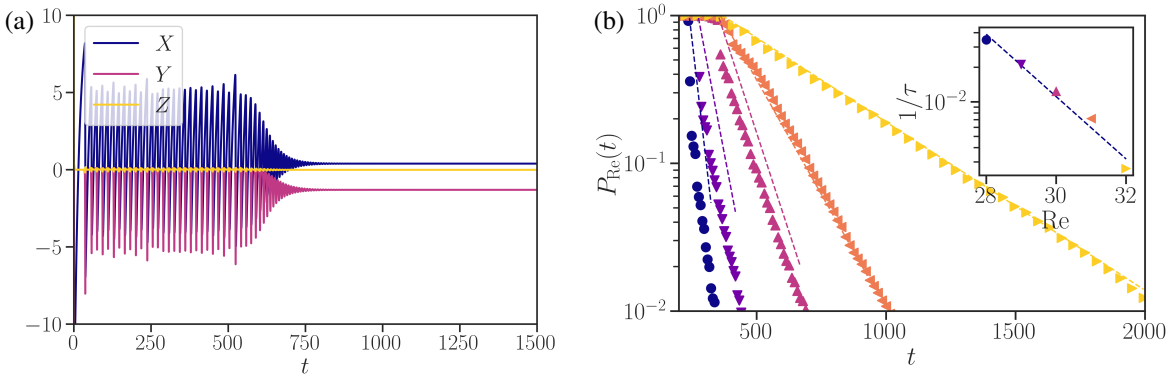

Figure 5. (a) Time series of (X,Y,Z) of the model (3) at $\mathrm{Re} = 32$ with a random initial condition. See main text for the parameter set-up. (b) Survival probability $P_{\mathrm{Re}}(t)$ of the transient chaos of the model (3) evaluated from 10,000 samples for each Re. The parameter set is the same as panel (a). Different symbols correspond to different values of Re. Dashed line denotes exponential fitting (4) using $0.01 \leq P_{\mathrm{Re}}(t) \leq 0.9$ data. Inset: Escape rate $1/\tau$ as a function of Re. Dashed line denotes the exponential fitting (5). Symbols are the same as the main plot.

CONCLUSIONS

We investigate the Quasi-Cyclic Behaviour (QCB) observed in a periodic box flow driven by the steady Taylor-Green forcing (2). We reveal that there is intrinsic periodicity in turbulent flow by phase-averaging the complex time series (Fig. 1 (d)), which is similar to the 3D periodic flow (3DPF) at low Re (Fig. 1 (b)). By conducting the mode-by-mode analysis of the 3DPF, we propose the three-equation model (3) describing the evolution of the velocity amplitude of the three distinct scales, namely forced, primary (energy-containing), and secondary (the rest) Fourier modes (Fig. 2). We fit the model parameters from the 3DPF to find the qualitatively similar periodic solutions (Fig. 4). The model exhibits permanent chaos at higher Re, which corresponds to statistically steady turbulence (Fig. 3). In a different parameter set-up, we find sudden relaminarisation of transient chaos (Fig. 5 (a)) with the exponential scaling of the survival probability (Fig. 5 (b)). We conclude that the proposed minimal model with only three variables contains fundamental properties of turbulence. We will further investigate the model analytically and numerically and its similarity with the existing model to present a complete picture of the model at the conference.

REFERENCES

Araki, Ryo, Bos, Wouter J. T. & Goto, Susumu 2022 Minimal modeling of the intrinsic cycle of turbulence driven by steady forcing. *arXiv preprint* .

Goto, Susumu, Saito, Yuta & Kawahara, Genta 2017 Hierarchy of antiparallel vortex tubes in spatially periodic turbulence at high Reynolds numbers. *Physical Review Fluids* **2** (6), 64603.

Linkmann, Moritz F. & Morozov, Alexander 2015 Sudden relaminarization and lifetimes in forced isotropic turbulence. *Physical Review Letters* **115** (13), 134502.

Lucas, Dan & Kerswell, Rich R 2017 Sustaining processes from recurrent flows in body-forced turbulence. *Journal of Fluid Mechanics* **817** (4), 178–205.

van Veen, Lennaert, Vela-Martín, Alberto & Kawahara, Genta 2019 Time-Periodic Inertial Range Dynamics. *Physical Review Letters* **123** (13), 134502.

Waleffe, Fabian 1997 On a self-sustaining process in shear flows. *Physics of Fluids* **9** (4), 883–900.